

Short Communication

A Novel Photoelectrochemical Assay for Cysteine Based on the Target-Induced Generation of Photosensitizer

Feng Li^{1,*}, Binbin Zhou^{2,*} and Wenbo Zhang³

¹ College of Chemistry and Chemical Engineering, Shangqiu Normal University, Shangqiu, Henan 476000, People's Republic of China

² Hunan Institute of Food Quality Supervision Inspection and Research, Building B, No. 238, Ave. Timesun, District Yuhua, Changsha, Hunan 410111, People's Republic of China

³ Nanyang No.2 High School, Zhongzhou Road, No. 142, Nanyang 473000, Henan, People's Republic of China

*E-mail: lifeng1985@tju.edu.cn, bbzhou1985@163.com

Received: 28 March 2018 / Accepted: 16 May 2018 / Published: 5 June 2018

A novel photoelectrochemical (PEC) assay was proposed for the specific detection of cysteine (Cys) based on the strategy of target-triggered generation of photosensitizer. The photosensitizer precursor, 1-(2,4-dinitrobenzenesulfonyl),2-dihydroxybenzene (**1**), was obtained by coupling 2,4-dinitrobenzenesulfonyl chloride with catechol (CA). In the presence of Cys, compound **1** can be specifically converted to CA which could coordinate on the surface of TiO₂ nanotubes (TiO₂ NTs) and act as effective photosensitizer. The resulted CA-decorated TiO₂ NTs displayed a significantly enhanced photocurrent response. Thus, an efficient Cys PEC assay was obtained with high sensitivity and selectivity. Moreover, the proposed strategy for the development of PEC assays by adapting the target-responsive photosensitizer precursor would provide a general format for versatile PEC sensing.

Keywords: Photoelectrochemical, TiO₂ nanotubes, Cysteine, Photosensitizer

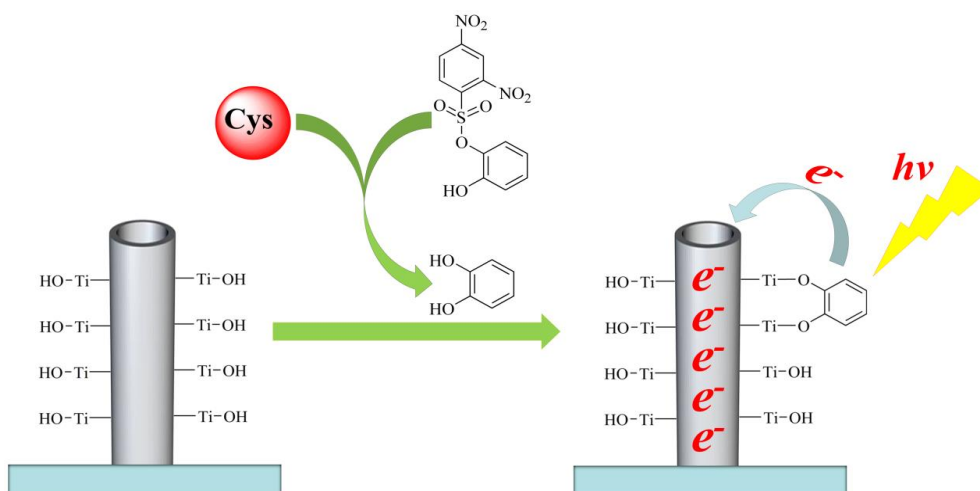
1. INTRODUCTION

As an essential amino acid and an important biothiol, cysteine (Cys) participates in many biological processes, such as protein synthesis, antioxidation, detoxification, signaling, cellular growth and death [1, 2]. On the other hand, abnormal level of Cys is implicated with a variety of diseases and syndromes, such as neurotoxicity, retarded growth rate, hair depigmentation, liver damage [3-5]. Thus,

the development of efficient methods for the detection of Cys is urgently required to further elucidate its biological roles.

Photoelectrochemical (PEC) sensing is a newly developing and rapidly expanding analytical technique [6-8]. Due to the separation of excitation source (light) and the recording signal (current) and the resulted low background, PEC assays displayed excellent sensitivity. Moreover, the PEC assays inherit the advantages of electrochemical methods [9-11], such as low cost, rapid analysis, and simple instrumentation. As a result, a large number of PEC sensors has been developed for various targets, such as enzymes [12], nucleic acids [13], proteins [14], metal ions [15, 16], and small molecules including cysteine [17-23]. But most these proposed PEC assays for cysteine are based on the direct oxidation of the target by the oxidized photosensitizers. Other reductive species in complex biological samples would interfere the photocurrent signal, and thus resulting inferior specificity of the assay. Previously, several strategies has been exploited to improve the selectivity of PEC assays, including adapting the specific antigen-antibody recognition [24], nucleic acids recognition [25], *in situ* introduction/generation of photosensitizers [26, 27]. The last strategy holds great potential for the development of high performance PEC sensors towards various analytes, as numerous photosensitizer precursors can be devised by properly introducing the recognition moiety of different target analytes.

Based on these above considerations, we reported herein a new PEC assay for the detection of Cys (shown in Scheme 1). TiO₂ nanotubes (TiO₂ NTs) electrode was firstly prepared by anodic oxidation of titanium foil. 1-(2,4-Dinitrobenzenesulfonyl),2-dihydroxybenzene (**1**) was designed and synthesized as a photosensitizer precursor for the recognition of Cys. The reaction of compound **1** with Cys would lead to the generation of catechol (CA) which can coordinate to the TiO₂ NTs electrode and serve as a photosensitizer. The resulted TiO₂ NTs-CA electrode could be effectively excited by visible light and generate a significantly increased photocurrent. The proposed PEC assay displayed high sensitivity and selectivity for Cys. Moreover, the proposed strategy of employing target-responsive photosensitizer precursor opens up new avenues for the construction of versatile PEC sensors.



Scheme 1. Schematic illustrating the sensing mechanism of the proposed PEC assay for Cys.

2. EXPERIMENTAL

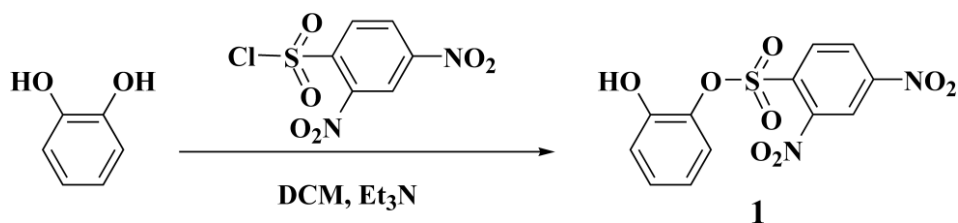
2.1 Chemicals and instruments

Titanium sheet was obtained from Sigma and was cleaned by sonicating it successively in acetone, ethanol, and deionized (DI) water, for 10 min each, followed by drying in an nitrogen stream. Other chemicals were analytical grade and received from commercial suppliers without further purification. The absorbance spectra were recorded with a Cary 60 UV–Vis spectrophotometer (Agilent Technologies, Santa Clara, USA). Mass spectrometry was performed on a Waters Xevo G2-S QToF™ mass spectrometer (Waters, Milford, MA, USA). Analytical HPLC was performed on a Waters ACQUITY BEH C18 column (2.1 × 50 mm, 1.7 μm, Agilent) with a Waters Acquity UPLC H-Class system (Milford, MA, USA). Flow rate was 0.5 mL/min. Detection wavelength was set at 280 nm. Eluent components were water (A) and acetonitrile (B). The mobile phase gradient was as follows: the proportion of phase B increased from 50 to 75% in 2 min.

2.2 Preparation of the TiO₂ Nanotubes

TiO₂ nanotubes were prepared by a well-established two-step anodization process [28, 29]. First, anodization was conducted under ambient conditions (50 V, 2 h) in a solution of 2 vol% H₂O and 0.3 wt % NH₄F in ethylene glycol. Ti foil and graphite sheet were used as the working electrode and counter electrode, respectively. The resultant Ti sheet were thoroughly washed by H₂O, dried with a stream of N₂, and vigorously sonicated in ethanol to remove the surface layer. Then, anodization was repeated again (50 V, 30 min) to prepare the TiO₂ NTs. The obtained TiO₂ NTs were subjected to the same washing and drying procedures and finally calcined in air (450 °C, 1 h) to afford the TiO₂ NTs electrode.

2.3 Synthesis of compound 1



Scheme 2. Synthetic route for compound 1.

Compound 1 can be facilely obtained through a one-step reaction. Briefly, to a solution of catechol (110 mg, 1.0 mmol) and 2,4-dinitrobenzenesulfonyl chloride (266 mg, 1.0 mmol) in dichloromethane (10 mL) was added triethylamine (121 mg, 1.2 mmol). The mixture was stirred at room temperature overnight. Then solvent was removed under reduced pressure and the obtained

residue was purified by column chromatography using dichloromethane/methanol (10/1, v/v) to afford the desired compound **1** as a white solid (282 mg, 83%).

2.4 Photoelectrochemical measurements

To a aqueous solution of compound **1** (1 mM, 1mL) was added with different concentrations of Cys, and reacted for 30 min at room temperature. During this process, compound **1** can be converted to CA, then TiO₂ NTs electrode was incubated with the above mixture for 10 min and gently rinsed with phosphate buffer. For PEC measurement, the obtained TiO₂ NTs-CA electrode was served as the work electrode, Pt wire and a saturated Ag/AgCl electrode as counter electrode and reference electrode, respectively. The electrolyte consisted of phosphate buffer (pH 7.4, 0.1 M) and 0.1 M ascorbic acid (AA), which acted as a sacrificial electron donor. The irradiation source was supplied by a fluorescence spectrophotometer (F7000, HITACHI, Tokyo, Japan). Photocurrent was measured on a DY2000 potentiostat instrument (Digi-IVY, Austin, TX). The bias voltage was set at 0 V.

3. RESULTS AND DISCUSSION

3.1 Characterization of TiO₂ NTs

The well-defined TiO₂ NTs was prepared by a two-step anodization approach. Figure 1 shows the SEM image of the as-obtained TiO₂ NTs, which exhibited a self-organized porous structure with good conformity in large scale. The magnified SEM image (Figure 1B) demonstrated that the average diameter of the nanotubes was ~100 nm with a wall thickness of ~10 nm. Figure 1C shows the cross-sectional image of the self-ordered porous TiO₂ NTs with a length of approximately 3.5 μm. Such well-aligned one-dimensional structure would allow efficient directional charge transport within the arrayed tubes.

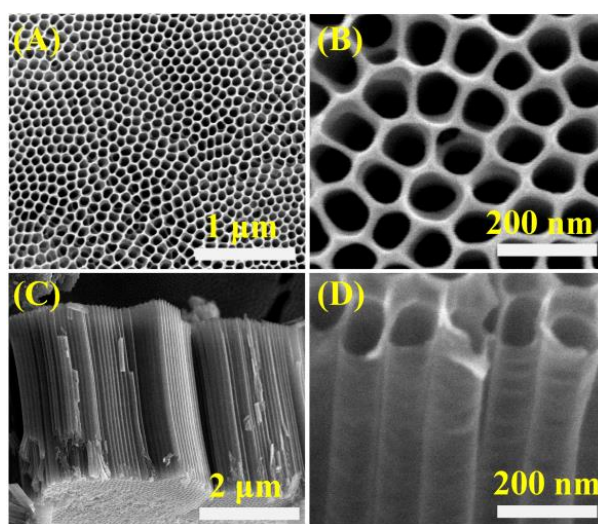
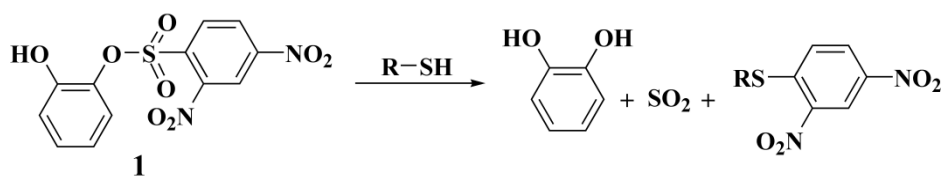


Figure 1. SEM images of TiO₂ NTs, A and B top view, C and D cross-sectional view.

3.2 studies on the reaction of compound **1** with Cys**Scheme 3.** The reaction of **1** with Cys.

As shown in Scheme 1, the sensing mechanism of the PEC assay relies on the reaction between **1** with Cys. Compound **1** features a 2,4-dinitrobenzenesulfonyl (DNBS) ester structure, which is a well-known reaction site for biothiols. We firstly inspected the feasibility of the reaction between **1** with Cys by UV-vis spectrometry and HPLC technique.

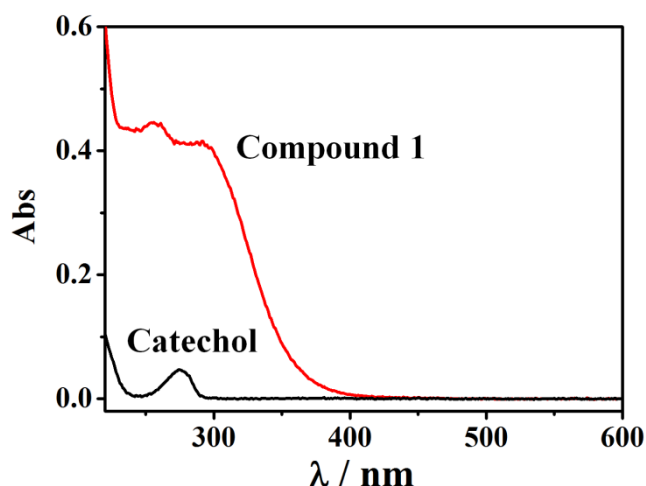
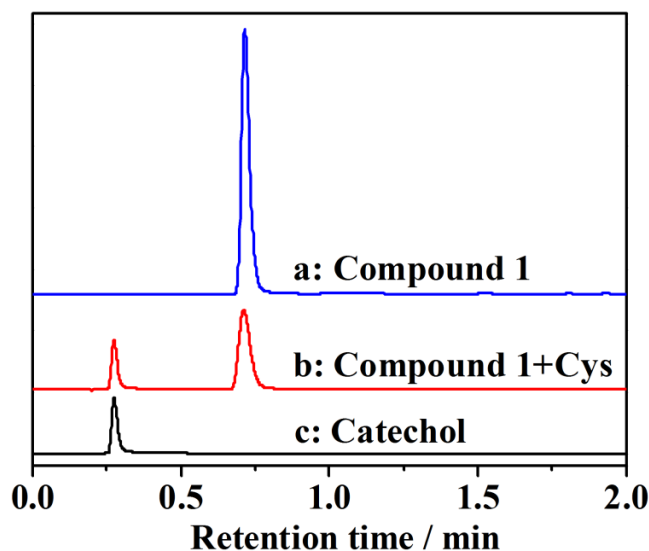
**Figure 2.** UV-vis absorption spectra of catechol (20 μM) and compound **1** (20 μM) in phosphate buffer (pH 7.4, 10 mM).**Figure 3.** HPLC chromatograms of compound **1** (curve a), **1** and Cys (curve b), and catechol (curve c). All the concentrations of **1**, Cys and catechol were 10 μM .

Figure 2 shows the absorption spectra of CA and compound **1**. CA displayed a weak absorption centered at 280 nm ($\epsilon_{280} = 2.47 \times 10^4$), while compound **1** has a relatively strong red-shifted absorption at 295 nm ($\epsilon_{295} = 2.04 \times 10^5$), which can be ascribed to the strong electron-withdrawing ability of DNBS and the resulting enhanced ICT (intramolecular charge transfer) effect within **1**. From the HPLC tests (Figure 3), it can be clearly seen that compound **1** displayed a single peak with R_t (retention time) at 0.71 min (Figure 3, curve a). After incubation with Cys, a new peak at 0.27 min was appeared (Figure 3, curve b), which was identical to that of CA (Figure 3, curve c). These results demonstrated that **1** can react with Cys to release CA.

3.3 Photoelectrochemical Measurements

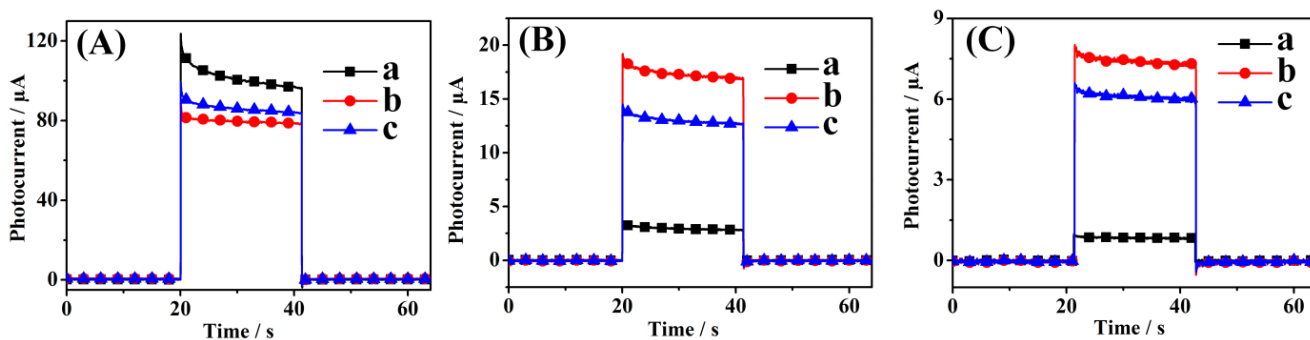


Figure 4. Photocurrent responses of the TiO₂ NTs electrode (curve a), TiO₂ NTs electrode incubating with CA (1 mM) (curve b), and TiO₂ NTs electrode incubating compound **1** (1 mM) and Cys (1 mM) (curve c), under different wavelengths of irradiation lights: A (350 nm), B (400 nm) and C (450 nm).

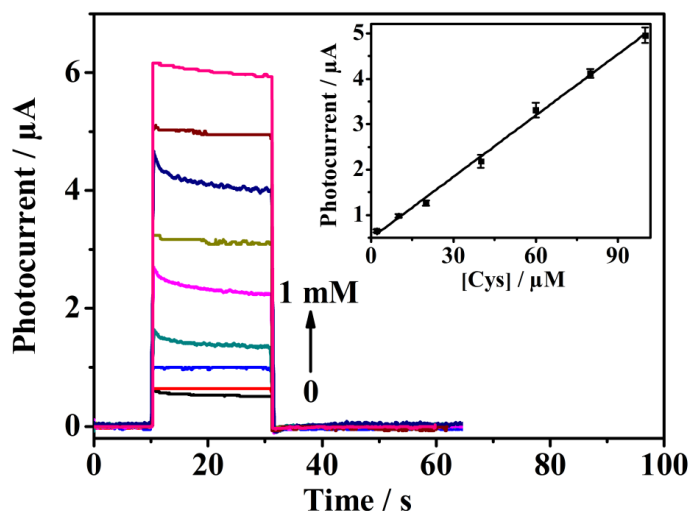


Figure 5. Photocurrent response of the PEC sensor for the detection of different concentrations of Cys (0, 2 μM, 10 μM, 20 μM, 40 μM, 60 μM, 80 μM, 100 μM, and 1 mM). Inset is the Calibration curve of the PEC sensor for Cys, error bars deriving from the standard deviation of three measurements.

The PEC responses of TiO₂ NTs electrode under various conditions were recorded (Figure 4). The TiO₂ NTs electrode alone displayed high photocurrent response under ultraviolet light irradiation (350 nm, Figure 4A, curve a), and only showed weak photocurrent while illuminated by visible light (Figure 4B and 4C, curves a), which can be ascribed to the intrinsic wide band gap of TiO₂ (3.2 eV, corresponding to ~390 nm). The TiO₂ NTs electrode treating with CA solution exhibited similar photocurrent response under ultraviolet light illumination (350 nm, Figure 4A, curve b), but displayed dramatically enhanced photocurrent when exciting by light with wavelength in the visible region (Figure 4B and 4C, curves b), which can be attributed to the formation of dopamine–Ti complex by the coordination of enediol ligands of CA to the surface Ti sites of TiO₂.

When treating the electrode with a mixture of compound **1** and Cys, similar photocurrent response behaviors compared to that of CA were also observed (Figure 4, curves c). To diminish the interference photocurrent of pristine TiO₂, we chose 450 nm as the excitation wavelength for the subsequent PEC tests.

We next exploited the PEC assay for the quantitative analysis of Cys. As shown in Figure 5, the photocurrents are increased along with the concentration of Cys. The calibration curve of photocurrent variation to different concentrations of Cys was also fitted (Figure 5, inset). The relative standard deviation at each concentration was less than 6%, indicating a favorable reproductivity of the assay. The dynamic range of Cys was found to be 2 ~ 100 μM with a correlation coefficient of 0.996, which can be expressed as $photocurrent/\mu A = 0.04494[Cys] (\mu M) + 0.4932$. The limit of detection (LOD) was calculated 0.65 μM (S/N = 3). This value is much lower than the contents of Cys in real samples (e.g. human serum).

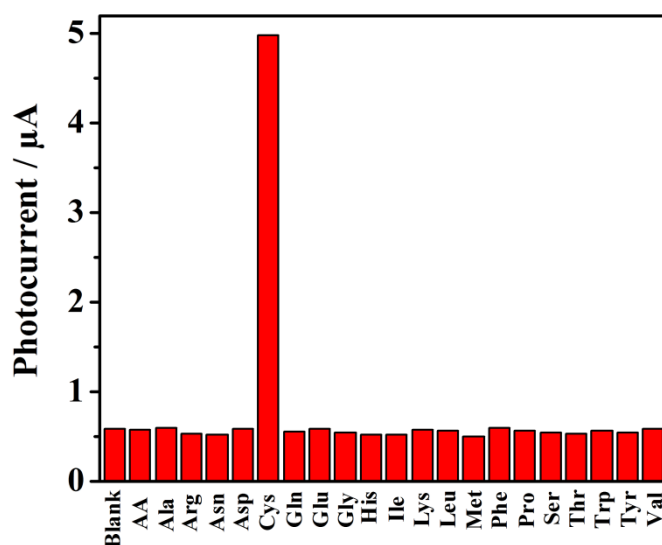


Figure 6. Photocurrent response of the PEC sensor upon incubating with a mixture of compound **1** (1 mM) and 100 μM each of ascorbic acid (AA) or 20 individual amino acids.

The selectivity of the assay to Cys was evaluated by testing these relevant species. From Figure 6, the interferences such as various amino acids and ascorbic acid (AA) showed negligible

photocurrent changes, indicating that the proposed assay possessed excellent ability against interference. Therefore, these results demonstrate a high selectivity of the proposed platform towards Cys.

The performances of the developed assay for Cys was compared with other recently reported PEC methods [17-21, 30-33] (shown in Table 1). Most of these reported PEC methods were based the direct oxidation of Cys at the interface of the photoanode, so other reductive species (i.e. ascorbic acid, dopamine, glucose, uric acid and etc.) may lead to the generation interference photocurrent. Our assays, which is based on the specific Cys-triggered formation of photosensitizer, should exhibit superior compared to other assays on the aspect of selectivity.

Table 1. Comparison of the main analytical performances between our assays and other reported methods for Cys sensing

Working Electrode	Linear range	LOD (μM)	Responding mode	Ref.
CuO–Cu ₂ O/GEC	0.2 – 10 μM	0.05 μM	Direct oxidation	[17]
CdS:Mn/RGO/ITO	0.1 μM – 20 mM	0.02 μM	Direct oxidation	[18]
TTA/TiO ₂ /FTO	1 – 200 μM	0.7 μM	Target-induced transformation of photosensitizer	[19]
S ²⁻ /CdS/ITO	1 – 100 μM	0.4 nM	Target-mediated desorption of electron donor	[20]
CdS–MV/Nafion/ITO	0.2 – 2.8 μM	0.1 μM	Direct oxidation	[21]
PPIX/WO ₃ –rGO/ITO	0.1 – 100 μM	25 nM	Direct oxidation	[30]
FTO	0.1 – 3 mM	50 μM	Direct oxidation	[31]
PTh/TiO ₂ /FTO	0.06 – 0.5 mM	12.6 μM	Direct oxidation	[32]
Au NPs/Bi ₄ NbO ₈ Cl/ITO	0.1 – 10 mM	10 μM	Direct oxidation	[33]
TiO ₂ /FTO	2 – 100 μM	0.65 μM	Target-induced formation of photosensitizer	This Work

Table 2. Determination of Cys in human serum sample

Spiked (μM)	Detected (μM) By our method	Detected (μM) By Ellman's assay	Recovery (%)	RSD (%)
0	235.6	213.4	--	3.8
100	332.7	317.5	97.1	5.4
200	425.1	414.6	94.8	4.2
500	714.9	703.8	95.9	3.1

To further demonstrate the feasibility of the proposed method for real sample analysis, we measured the Cys content and its recoveries in a human serum sample. The concentration of Cys in human serum was determined to be 235.6 μM , which is in good agreement with the previously reported results [34]. This value also compares reasonably well with that we determined by UV-vis spectrometric analysis using the Ellman's reagent (213.4 μM) [35]. Both our method and the UV-vis spectrometry produced values that are well within the range of total serum Cys (174 ~ 378 μM) reported in the literature [36]. The accuracy of the assay was further evaluated by calculating recoveries of spiked Cys in human serum sample (Table 2). The recovery of Cys at each concentration was statistically close to 100%, and all the determined concentrations were in good agreement with the values obtained from the standard Ellman's assay. Therefore, our method is accurate and applicable for the detection of Cys in a real sample.

4. CONCLUSION

In summary, a novel strategy was proposed for the construction of PEC assay by employing the target-responsive photosensitizer precursor. DNBS substituted CA (**1**) was designed as model a photosensitizer precursor for the recognition of Cys. The analyte can specifically react with **1** to release CA which can coordinate to the surface of TiO_2 NTs to form dopamine-Ti complex and generate sensitive photocurrent response under visible light illumination. The proposed PEC sensor exhibited high selectivity and sensitivity with a low detection limit of 0.65 μM . Moreover, the proposed sensing strategy can be further applied for the development of versatile PEC sensors for various targets.

ACKNOWLEDGMENTS

This work is financially supported by the National Natural Science Foundation of China (21502111) and the Natural Science Foundation of Hunan Province of China (2018JJ3300)

References

1. X. Chen, Y. Zhou, X. Peng and J. Yoon, *Chem. Soc. Rev.*, 39 (2010) 2120-2135.
2. Z. A. Wood, E. Schröder, J. Robin Harris and L. B. Poole, *Trends Biochem. Sci.*, 28 (2003) 32-40.
3. S. Zhang, C.-N. Ong and H.-M. Shen, *Cancer letters*, 208 (2004) 143-153.
4. V. Gazit, R. Ben-Abraham, R. Coleman, A. Weizman and Y. Katz, *Amino Acids*, 26 (2004) 163-168.
5. Y. Hao, D. Xiong, L. Wang, W. Chen, B. Zhou and Y.-N. Liu, *Talanta*, 115 (2013) 253-257.
6. W.-W. Zhao, J.-J. Xu and H.-Y. Chen, *Chem. Rev.*, 114 (2014) 7421-7441.
7. W.-W. Zhao, J.-J. Xu and H.-Y. Chen, *Chem. Soc. Rev.*, 44 (2015) 729-741.
8. W.-W. Zhao, J.-J. Xu and H.-Y. Chen, *Anal. Chem.*, 90 (2018) 615-627.
9. N. Xia, P. Peng, S. Wang, J. Du, G. Zhu, W. Du and L. Liu, *Sensor. Actuat B-Chem.*, 232 (2016) 557-563.
10. N. Xia, X. Wang, J. Yu, Y. Wu, S. Cheng, Y. Xing and L. Liu, *Sensor. Actuat B-Chem.*, 239 (2017) 834-840.
11. N. Xia, Z. Chen, Y. Liu, H. Ren and L. Liu, *Sensor. Actuat B-Chem.*, 243 (2017) 784-791.
12. V. Pardo-Yissar, E. Katz, J. Wasserman and I. Willner, *J. Am. Chem. Soc.*, 125 (2003) 622-623.

13. Y. Wu, B. Zhang and L.-H. Guo, *Anal. Chem.*, 85 (2013) 6908-6914.
14. P. Da, W. Li, X. Lin, Y. Wang, J. Tang and G. Zheng, *Anal. Chem.*, 86 (2014) 6633-6639.
15. W.-W. Zhao, J.-J. Xu and H.-Y. Chen, *The Analyst*, 141 (2016) 4262-4271.
16. N. Xia, Y. Q. Hao, L. J. Zhao and W. J. Hou, *Int. J. Electrochem. Sci.*, 11 (2016) 9462-9470.
17. Y. Zhu, Z. Xu, K. Yan, H. Zhao and J. Zhang, *ACS Appl. Mater. Inter.*, 9 (2017) 40452-40460.
18. Q. Shen, X. Shi, M. Fan, L. Han, L. Wang and Q. Fan, *J. Electroanal. Chem.*, 759 (2015) 61-66.
19. S. Wu, H. Song, J. Song, C. He, J. Ni, Y. Zhao and X. Wang, *Anal. Chem.*, 86 (2014) 5922-5928.
20. L. Zhang, Y. Hao, X. Wang, Y. Long, A. Ramos, D. Jiang, X. Ma, Q. Lin and F. Zhou, *Electroanalysis*, 27 (2015) 1899-1905.
21. Y. T. Long, C. Kong, D. W. Li, Y. Li, S. Chowdhury and H. Tian, *Small*, 7 (2011) 1624-1628.
22. G. M. Yang, X. L. Chen, Q. S. Pan, W. Liu and F. Q. Zhao, *Int. J. Electrochem. Sci.*, 12 (2017) 7272-7286.
23. Y. Hao, Y. Cui, P. Qu, W. Sun, S. Liu, Y. Zhang, D. Li, F. Zhang and M. Xu, *Electrochim. Acta*, 259 (2018) 179-187.
24. W.-W. Zhao, Z.-Y. Ma, D.-Y. Yan, J.-J. Xu and H.-Y. Chen, *Anal. Chem.*, 84 (2012) 10518-10521.
25. X. Zeng, S. Ma, J. Bao, W. Tu and Z. Dai, *Anal. Chem.*, 85 (2013) 11720-11724.
26. C. Li, H. Wang, J. Shen and B. Tang, *Anal. Chem.*, 87 (2015) 4283-4291.
27. J. Li, W. Tu, H. Li, J. Bao and Z. Dai, *Chem. Commun.*, 50 (2014) 2108-2110.
28. D. R. Baker and P. V. Kamat, *J. Phys. Chem. C*, 113 (2009) 17967-17972.
29. F.-X. Xiao, Z. Zeng and B. Liu, *J. Am. Chem. Soc.*, 137 (2015) 10735-10744.
30. B. Sun, K. Zhang, L. Chen, L. Guo and S. Ai, *Biosens. Bioelectron.*, 44 (2013) 48-51.
31. S. Mu and Q. Shi, *Electrochim. Acta*, 195 (2016) 59-67.
32. Y. Wang, W. Wang, S. Wang, W. Chu, T. Wei, H. Tao, C. Zhang and Y. Sun, *Sensor. Actuat B-Chem.*, 232 (2016) 448-453.
33. Y.-F. Ruan, N. Zhang, Y.-C. Zhu, W.-W. Zhao, J.-J. Xu and H.-Y. Chen, *Anal. Chem.*, 89 (2017) 7869-7875.
34. D. W. Jacobsen, V. J. Gatautis, R. Green, K. Robinson, S. R. Savon, M. Secic, J. Ji, J. M. Otto and L. M. Taylor, *Clin. Chem.*, 40 (1994) 873-881.
35. G. L. Ellman, *Arch. Biochem. Biophys.*, 82 (1959) 70-77.
36. S. P. Stabler, P. D. Marcell, E. R. Podell and R. H. Allen, *Anal. Biochem.*, 162 (1987) 185-196.